

## Brief Communication

# External globus pallidus stimulation modulates brain connectivity in Huntington's disease

Noémie Ligot<sup>1,2</sup>, Pierre Krystkowiak<sup>3,11</sup>, Clémence Simonin<sup>4,5,6,7,11</sup>, Serge Goldman<sup>1,2</sup>, Philippe Peigneux<sup>8</sup>, John Van Naemen<sup>2</sup>, Michel Monclus<sup>2</sup>, Simon Frédéric Lacroix<sup>2</sup>, David Devos<sup>4,5,6,7</sup>, Kathy Dujardin<sup>4,5,6,7</sup>, Christine Delmaire<sup>4,5,6,7</sup>, Eric Bardinet<sup>9</sup>, Arnaud Delval<sup>4,5,6,7</sup>, Marie Dellioux<sup>4,5,6,7</sup>, Luc Defebvre<sup>4,5,6,7</sup>, Jerome Yelnik<sup>9</sup>, Serge Blond<sup>4,5,6,10</sup>, Alain Destée<sup>4,5,6,7</sup> and Xavier De Tiège<sup>1</sup>

<sup>1</sup>Laboratoire de Cartographie Fonctionnelle du Cerveau, ULB-Hôpital Erasme, Université Libre de Bruxelles, Brussels, Belgium; <sup>2</sup>PET/Biomedical Cyclotron Unit, ULB-Hôpital Erasme, Université Libre de Bruxelles, Brussels, Belgium; <sup>3</sup>Department of Neurology, CNRS UMR 8160, Amiens University Hospital, Amiens, France; <sup>4</sup>Université Lille Nord de France, Lille, France; <sup>5</sup>UDSL, Lille, France; <sup>6</sup>CHU Lille, Lille, France; <sup>7</sup>EA 2683 MENRT and Movement Disorder Unit, Lille, France; <sup>8</sup>Department of Neuropsychology and Functional Neuroimaging Unit, Université Libre de Bruxelles, Brussels, Belgium; <sup>9</sup>INSERM U679, Groupe Hospitalier La Pitié-Salpêtrière, Paris, France; <sup>10</sup>Department EA 2683 MENRT and Department of Neurosurgery, CHU Lille, Lille, France

**Positron emission tomography with O-15-labeled water was used to study at rest the neurophysiological effects of bilateral external globus pallidus (GPe) deep brain stimulation in patients with Huntington's disease (HD). Five patients were compared with a control group in the on and off states of the stimulator. External globus pallidus stimulation decreased neuronal activity and modulated cerebral connectivity within the basal ganglia-thalamocortical circuitry, the sensorimotor, and the default-mode networks. These data indicate that GPe stimulation modulates functional integration in HD patients in accordance with the basal ganglia-thalamocortical circuit model.**

*Journal of Cerebral Blood Flow & Metabolism* advance online publication, 20 October 2010; doi:10.1038/jcbfm.2010.186

**Keywords:** basal ganglia; deep brain stimulation; default-mode network; Huntington's disease; positron emission tomography

## Introduction

Huntington's disease (HD) is an autosomal dominant neurodegenerative disease resulting in progressive impairments in motor function, cognition, and behavior. A characteristic feature of HD is the presence of chorea, which is related to striatal neuron degeneration. A standard model proposes that the striatum forms the input nucleus of a basal ganglia-thalamocortical circuitry integrating cortical

and thalamic afferents (Alexander *et al*, 1986). Striatal projection neurons target either the external globus pallidus (GPe) (indirect pathway) or the internal globus pallidus (direct pathway), projecting to the motor cortex through the thalamus. Activation of the direct pathway disinhibits the thalamus, thereby increasing thalamocortical activity, whereas activation of the indirect pathway further inhibits thalamocortical neurons. In HD, the preferential loss of striatal neurons contributing to the indirect pathway leads to reduced inhibition of GPe and excessive inhibition of the subthalamic nucleus, thus concurring to hyperstimulation of the motor network and chorea (DeLong, 2000). Therefore, a potential therapeutic approach for HD hyperkinetic symptoms could consist in GPe inhibitory stimulation to indirectly reduce thalamocortical hyperactivity, as already suggested by animal experiments (Temel *et al*, 2006). This stimulation is also expected to alleviate disturbances in the dorsolateral prefrontal and lateral orbitofrontal circuits responsible for the

Correspondence: Dr N Ligot, Laboratoire de Cartographie Fonctionnelle du Cerveau, ULB-Hôpital Erasme, 808 Route de Lennik, 1070 Brussels, Belgium.  
E-mail: nligot@ulb.ac.be

<sup>11</sup>These authors contributed equally to this work.

This study was supported by research grants of the FRS-FNRS (Belgium) and by PHRC 2004/R1905 (France) and by Adrinord (Association pour le Développement de la Recherche et de l'Innovation dans le NORD PAS DE CALAIS).

Received 4 June 2010; revised 25 August 2010; accepted 15 September 2010

cognitive and behavioral symptoms in HD (Alexander *et al*, 1986; DeLong, 2000; Temel *et al*, 2006).

In a group of HD patients included in a clinical trial on bilateral high-frequency deep brain stimulation (DBS) of GPe (GPe-DBS), we used positron emission tomography (PET) with oxygen-15-labeled water ( $H_2^{15}O$ ) to study the neurophysiological effects of GPe-DBS at rest. We characterized the changes in brain perfusion and effective connectivity associated with GPe-DBS.

## Materials and methods

### Patients

Five right-handed symptomatic HD patients with GPe-DBS (3 women; age range: 41 to 60 years) and 15 right-handed healthy adult volunteers (10 women; mean age: 40.3 years; range: 25 to 60 years) gave informed consent to participate in the clinical and imaging studies approved by the institutional ethics committees. Patients with HD were genetically confirmed (range of CAG repeats: 41 to 53), their symptoms appeared 2 to 5 years before the present investigation, and the time between electrode implantation and PET ranged from 12 to 19 months. Patients' total functional capacity scores ranged from 10 to 12 (Shoulson and Fahn, 1979) (Supplementary Information).

### Positron Emission Tomography Data Acquisition and Analysis

Subjects were scanned with a Siemens ECAT EXACT HR + tomograph using automatic administration of repetitive  $H_2^{15}O$  bolus injection and image acquisition procedure as described elsewhere (Lipschutz *et al*, 2002). Control participants were scanned twice in eye-closed rest during a single imaging session. Patients with HD had two imaging sessions in identical conditions (two scans in eye-closed rest) with a time interval of 7 days, respectively, with the GPe stimulator switched on (on state) and switched off (off state). Patient and PET investigators were blinded to the stimulator status, which was randomly set 7

days before each PET session to ensure investigation in stabilized motor and cognitive status, based on known physiologic effects of DBS (Temperli *et al*, 2003). Random design was used to control for test-retest effects. Clinical stimulation parameters were kept unchanged (frequency: 130 Hz; voltage: 1 to 3 V; pulse width: 60 to 90 microseconds).

Positron emission tomography data were preprocessed and analyzed using the voxel-based statistical parametric mapping method (SPM8, Wellcome Department of Imaging Neuroscience, London, UK). Images were spatially realigned, normalized, and smoothed using a 16-mm full-width half-maximum isotropic Gaussian kernel. Global flow adjustment was performed by proportional scaling.

First, group-level subtractive analyses compared patients in the on and off states, and each state with control PET data. For these analyses, t-contrasts identified brain regions showing a significant decrease or increase in regional cerebral blood flow (rCBF). Thereafter, rCBF changes characterizing the on state in HD patients were identified in the comparison between on state and controls, masked exclusively by the comparison between off state and controls.

Finally, we performed effective connectivity analyses using pathophysiological interaction (PPI), adapted from psychophysiological interaction (De Tiege *et al*, 2004). In this study, PPI analyses were used to search in HD patients for GPe stimulation-induced changes in the contribution of a brain area to the level of rCBF in another brain area. Pathophysiological interaction analyses were conducted under the *a priori* hypothesis of stimulation-induced changes in effective connectivity in the basal ganglia-thalamocortical and motor circuits. In practice, voxels of interest were selected bilaterally in three nodes of the basal ganglia-thalamocortical circuits: the thalamus, globus pallidus (GP), and primary motor cortex (PMC). The signal in the selected voxels was used as a covariate of interest centered around condition means and interacting with each condition. These covariates of interest were introduced in separate design matrices including the patients's scans grouped by on and off conditions. Thereafter, PPI analyses identified, throughout the patients's brain, the regions showing stimulation-related differences in modulation with the considered voxels.

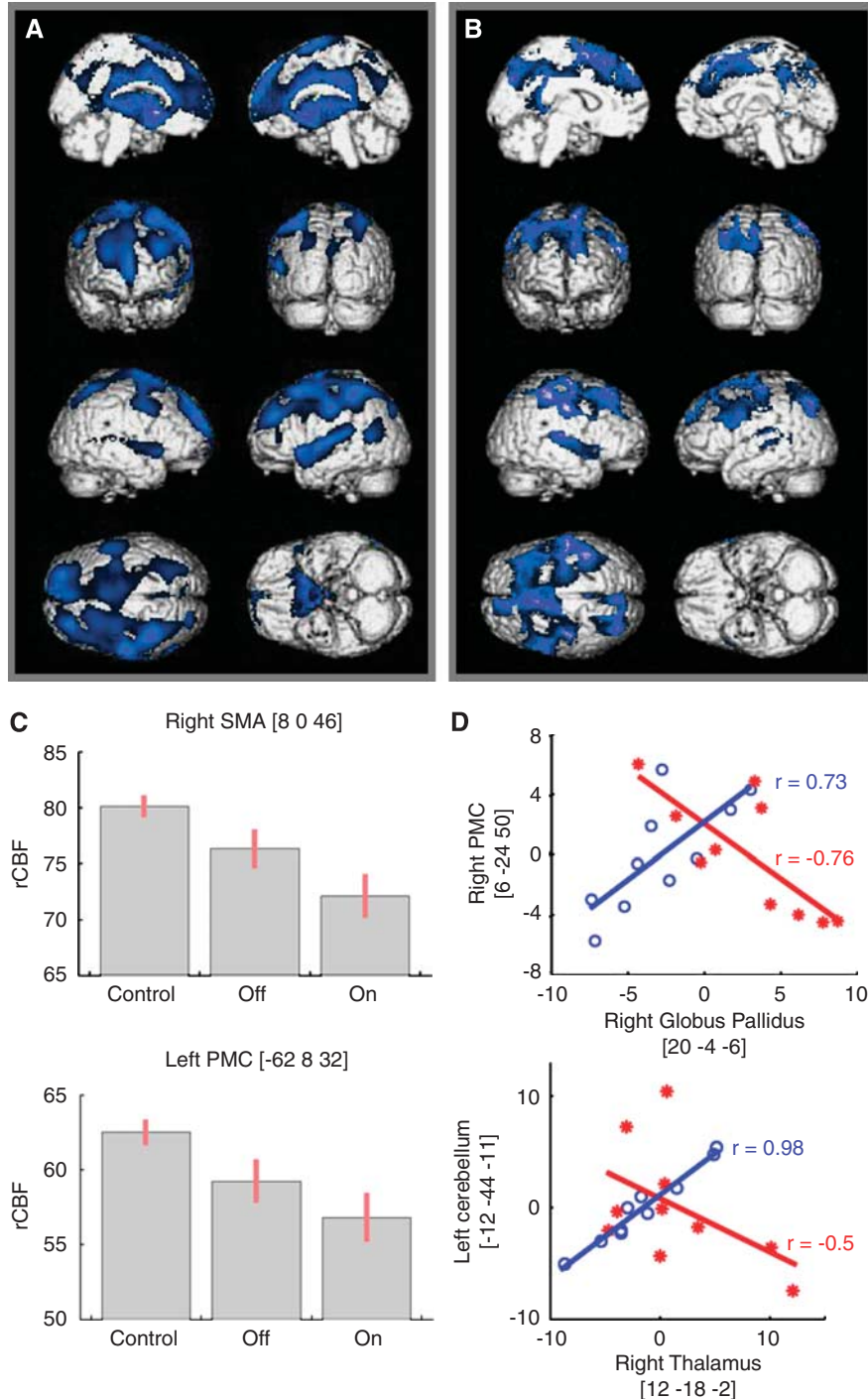
**Figure 1** Regional cerebral blood flow and effective connectivity changes induced by GPe stimulation in patients with Huntington's disease. **(A and B)** Regional cerebral blood flow (rCBF) changes observed in off- and on-stimulation states in patients with Huntington's disease (HD). Results are displayed at uncorrected  $P < 0.001$  thresholds. **(A)** Comparison between the off state and the control group showing significant rCBF decrease in the basal ganglia (the globus pallidus, putamen, and thalamus) and in the fronto-parieto-temporal cortical regions involving the primary sensori-motor cortices, the supplementary motor areas, the premotor cortices, dorsolateral prefrontal cortices, superior temporal gyri, the precuneus bilaterally, and the anterior and posterior cingular cortices. **(B)** Further significant rCBF decreases in the on state in the sensori-motor network (primary sensori-motor cortices, supplementary motor areas, and premotor cortices), the anterior cingular cortices and some other regions of the default-mode network (precuneus and posterior cingular cortex bilaterally), the superior temporal gyri, and prefrontal regions (dorsolateral prefrontal cortices and frontal eye fields). These results were obtained by the comparison between the on state and controls, masked exclusively by the comparison between the off state and controls. **(C)** Box plot depicting the mean rCBF at the peak voxel in the right SMA (upper figure) and in the left PMC (lower figure) in the control group and in the patient group in the on and off states of the stimulator. The mean rCBF is decreased in the selected brain areas in the patient group in the off state compared with the control group and is further decreased in the patient group in the on state compared with the off state. **(D)** Examples of typical modulation of basal ganglia-thalamocortical and cerebello-thalamo-cortical connectivity by external globus pallidus (GPe) stimulation in HD. Regression plot of the rCBF between the right globus pallidus (seed region) and the right primary motor cortex (upper figure) and between the right thalamus (seed region) and the left cerebellum (lower figure) in HD patients, as a function of GPe stimulation (on state: red stars; off state: blue circles). These plots present data for the two scans obtained in each state, in each patient. They illustrate GPe stimulation-induced modulation in effective connectivity between these two seed regions and cortical and cerebellar areas. PMC, primary motor cortex; SMA, supplementary motor area.

All results of SPM analyses were considered significant at  $P < 0.05$  corrected for multiple comparisons over the entire brain volume ( $P^{\text{corrFW}} < 0.05$ ) (De Tiege *et al*, 2004). Exclusive masking analyses were performed using an uncorrected mask  $P$ -value and a height threshold at 0.001. For PPI analyses, based on the *a priori* hypothesis of stimulation-induced changes in effective connectivity within the basal ganglia-thalamocortical and motor circuits, we also considered the voxels included in these regions as significant at small volume-corrected  $P < 0.05$  ( $P^{\text{corrSVC}} < 0.05$ , 10-mm radius spherical volume of interest).

## Results

### Regional Cerebral Blood Flow Changes During Resting State in Huntington's Disease Patients

Compared with controls, the off state was characterized by a significant relative rCBF decrease in the basal ganglia (GP, putamen, and thalamus) and in the fronto-parieto-temporal cortical regions involving primary sensori-motor cortices, supplementary motor areas, premotor cortices, dorsolateral prefrontal



cortices, superior temporal gyri, insula, precuneus, and anterior and posterior (PCC) cingulate cortices (Figure 1A). A significant relative increase in rCBF was found in the cerebellum.

Exclusive masking analyses revealed in the on state a further significant rCBF decrease in the sensorimotor network (primary sensori-motor cortices, supplementary motor areas, premotor cortices), the anterior cingulate cortex, and in other regions of the default-mode network (DMN) (precuneus and PCC), the superior temporal gyri, and prefrontal regions (dorsolateral prefrontal cortices, frontal eye fields) (Figures 1B and 1C). Masking analyses revealed no significant rCBF increase in the on state compared with the off state. Direct comparisons of HD patients in the on and off states did not reach significance.

### External Globus Pallidus Stimulation-Induced Changes in Cerebral Connectivity in Huntington's Disease Patients

Pathophysiological interaction analyses using thalamic seed voxels showed significant GPe-DBS-induced changes in effective connectivity with the

PMC and the cerebellum. Indeed, GPe-DBS reversed the correlation directionality between the thalami and PMC from negative in the off state to positive in the on state, and conversely for the thalami and cerebellum (Table 1, Figure 1D).

Pathophysiological interaction analyses using GP seed voxels showed significant GPe-DBS-induced changes in effective connectivity with the dorsolateral prefrontal cortices and primary sensori-motor cortices bilaterally (Figure 1D). Moreover, with the seed voxel in the right GP, PPI analyses additionally disclosed a significant change in effective connectivity with PCC and precuneus bilaterally. Indeed, GPe-DBS reversed the correlation directionality between GP and dorsolateral prefrontal cortices from negative in the off state to positive in the on state, and conversely, for GP and primary sensori-motor cortices, PCC, and precuneus bilaterally (Table 1).

Pathophysiological interaction analyses using seed PMC seed voxels showed that GPe-DBS induced a significant change in effective connectivity with supplementary motor areas bilaterally, with a correlation directionality reversal from negative in the off state to positive in the on state (Table 1).

**Table 1** Pathophysiological interaction (PPI) analyses showing GPe stimulation-induced changes in cerebral connectivity in Huntington's disease patients

| Region | Seed voxel |     |    | Voxels showing significant PPI |     |     |     |                    |       |       |    |       |       |      |
|--------|------------|-----|----|--------------------------------|-----|-----|-----|--------------------|-------|-------|----|-------|-------|------|
|        | Talairach  |     |    | Talairach                      |     |     |     | P-values           | r off | r on  |    |       |       |      |
|        | x          | y   | z  | Region                         | x   | y   | z   |                    |       |       |    |       |       |      |
| L Thal | -10        | -18 | -1 | L PMC                          | -48 | -12 | 62  | 0.006 <sup>a</sup> | -0.63 | 0.59  |    |       |       |      |
|        |            |     |    | R PMC                          | 48  | -12 | 54  | 0.013 <sup>a</sup> | -0.69 | 0.55  |    |       |       |      |
|        |            |     |    | L C                            | -14 | -36 | 18  | 0.018 <sup>a</sup> | 0.71  | -0.43 |    |       |       |      |
|        |            |     |    | R C                            | 10  | -50 | -40 | 0.007              | 0.83  | -0.74 |    |       |       |      |
| R Thal | 12         | -18 | -2 | L PMC                          | -52 | 0   | 44  | 0.018 <sup>a</sup> | -0.67 | 0.62  |    |       |       |      |
|        |            |     |    | L C                            | -12 | -44 | -11 | 0.001 <sup>a</sup> | 0.98  | -0.5  |    |       |       |      |
|        |            |     |    | R C                            | 16  | -72 | -20 | 0.020 <sup>a</sup> | 0.82  | -0.68 |    |       |       |      |
|        |            |     |    | R DLPFC                        | 36  | 50  | 26  | 0.000 <sup>a</sup> | -0.70 | 0.82  |    |       |       |      |
| L GP   | -20        | 4   | -6 | L DLPFC                        | -28 | 42  | 50  | 0.001 <sup>a</sup> | -0.66 | 0.74  |    |       |       |      |
|        |            |     |    | L PMC                          | -68 | 8   | 24  | 0.010 <sup>a</sup> | 0.64  | -0.83 |    |       |       |      |
|        |            |     |    | R PMC                          | 40  | 0   | 20  | 0.017 <sup>a</sup> | 0.54  | -0.63 |    |       |       |      |
|        |            |     |    | R PSC                          | 64  | -2  | 34  | 0.037 <sup>a</sup> | 0.59  | -0.64 |    |       |       |      |
|        |            |     |    | L PSC                          | -68 | 8   | 24  | 0.010 <sup>a</sup> | 0.64  | -0.83 |    |       |       |      |
|        |            |     |    | R GP                           | 20  | -4  | -6  | L DLPFC            | -14   | 64    | 22 | 0.019 | -0.89 | 0.75 |
|        |            |     |    | R DLPFC                        | 2   | 66  | 8   | 0.005 <sup>a</sup> | -0.80 | 0.76  |    |       |       |      |
|        |            |     |    | L PMC                          | -24 | -8  | 72  | 0.043 <sup>a</sup> | 0.88  | -0.54 |    |       |       |      |
| R GP   | 20         | -4  | -6 | R PMC                          | 6   | -24 | 50  | 0.006 <sup>a</sup> | 0.73  | -0.76 |    |       |       |      |
|        |            |     |    | L PSC                          | -18 | -44 | 50  | 0.009 <sup>a</sup> | 0.86  | -0.64 |    |       |       |      |
|        |            |     |    | R PSC                          | 6   | -30 | 80  | 0.013 <sup>a</sup> | 0.86  | -0.64 |    |       |       |      |
|        |            |     |    | L PCC                          | -4  | -52 | 30  | 0.024              | 0.86  | -0.78 |    |       |       |      |
|        |            |     |    | R PCC                          | 2   | -38 | 42  | 0.011 <sup>a</sup> | 0.76  | -0.73 |    |       |       |      |
|        |            |     |    | L PCu                          | -14 | -42 | 46  | 0.010 <sup>a</sup> | 0.81  | -0.66 |    |       |       |      |
|        |            |     |    | R PCu                          | 0   | -54 | 16  | 0.006 <sup>a</sup> | 0.71  | -0.73 |    |       |       |      |
|        |            |     |    | L SMA                          | -8  | -2  | 78  | 0.005 <sup>a</sup> | -0.73 | 0.71  |    |       |       |      |
| L PMC  | -42        | -18 | 66 | R SMA                          | 6   | -4  | 78  | 0.002 <sup>a</sup> | -0.79 | 0.78  |    |       |       |      |
|        |            |     |    | L SMA                          | -18 | -24 | 58  | 0.043 <sup>a</sup> | -0.73 | 0.62  |    |       |       |      |
|        |            |     |    | R SMA                          | 10  | 4   | 48  | 0.006 <sup>a</sup> | -0.85 | 0.46  |    |       |       |      |
|        |            |     |    | R SMA                          | 10  | 4   | 48  | 0.006 <sup>a</sup> | -0.85 | 0.46  |    |       |       |      |

C, cerebellum; DLPFC, dorsolateral prefrontal cortex; HD, Huntington's disease; GP, globus pallidus; GPe, external globus pallidus; L, left; PCC, posterior cingulate cortex; PCu, precuneus; PMC, primary motor cortex; PSC, primary somatosensory cortex; R, right; SMA, supplementary motor area; Thal, thalamus.  
<sup>a</sup>,  $P_{\text{corrSVC}}$ ; r off: Pearson's correlation coefficient between seed voxel and identified area in the off state; r on: Pearson's correlation coefficient between seed voxel and identified area in the on state.



## Discussion

This neuroimaging study shows that GPe-DBS decreases neuronal activity in the resting state and modulates connectivity within the basal ganglia-thalamocortical circuits, the motor network, and the DMN in patients with HD.

With the brain stimulator switched off, patients showed widespread cortico-subcortical rCBF decrease, with an anatomic distribution concordant with previous studies on HD patients (Weeks *et al*, 1997). Further rCBF decrease induced by GPe-DBS in the sensori-motor network, the anterior cingulate cortex, and the prefrontal regions is in line with the standard model of the basal ganglia-thalamocortical circuits that drove the choice of GPe as a site of therapeutic electrostimulation in HD (Alexander *et al*, 1986; DeLong, 2000). Thus, this imaging study in HD patients substantiates the physiologic model of the basal ganglia. Moreover, GPe-DBS modulates cerebral connectivity involving three major nodes of the basal ganglia-thalamocortical circuits, namely the thalamus, GPe, and PMC. This modulation leads to a connectivity pattern consistent with the standard model of the basal ganglia-thalamocortical circuits and data obtained in healthy subjects using PET or functional magnetic resonance imaging (Di Martino *et al*, 2008; Kim *et al*, 2009; Postuma and Dagher, 2006). These changes in effective connectivity observed in the on state provide some insight into the rCBF decrease found in brain regions under the indirect influence of GPe activity. They further support the choice of GPe as a therapeutic target for inhibitory DBS in HD. Neurologic confirmation within the framework of our clinical trial is required to confirm the actual value of such a therapeutic strategy.

Whatever the state of the stimulator, we found increased cerebellar rCBF, which might be attributed to the normalization process, highlighting variations relative to global cerebral perfusion. Indeed, a diffuse reduction of activity in the cerebral hemispheres, relative to the cerebellum, is expected in HD. Although this normalization effect imposes caution in the interpretation of effective connectivity changes with the cerebellum, it can hardly account for the observed inversion of the correlation between the thalami and the cerebellum from the off to the on state in HD patients. It must be noted that the connectivity pattern found between these structures is in line both with their established anatomic relationship within the cerebello-thalamo-cortical pathway and with a recent connectivity study on this pathway (Krienen and Buckner, 2009).

The DMN is defined as a set of brain regions that manifest greater activity during resting states as compared with goal-directed behaviors. This network prominently includes frontal regions along the midline, lateral, and medial parietal regions extending into the posterior cingulate and retrosplenial cortex, and the medial temporal lobes (Gusnard and

Raichle, 2001). Here, we found in the HD framework that GPe-DBS decreased neuronal activity in the PCC and the precuneus that are part of the DMN, in line with previous reports of connectivity between nodes of the basal ganglia-thalamocortical circuitry and the DMN in healthy subjects (Cavanna and Trimble, 2006; Gusnard and Raichle, 2001; Marchand *et al*, 2007). Moreover, changes in effective connectivity observed between GPe and both PCC and precuneus during GPe stimulation further support some degree of functional integration between these major networks (Marchand *et al*, 2007). These findings indicate that GPe-DBS effects in HD might extend beyond the motor pathways.

In conclusion, this neuroimaging study provides neurophysiological evidences supporting GPe as a therapeutic target for DBS strategies in HD.

## Acknowledgements

Noémie Ligot is 'clinicien chercheur doctorant' and Xavier De Tiège is 'clinicien chercheur spécialiste' at the 'Fonds de Recherche Scientifique' (FRS-FNRS, Belgium).

## Disclosure/conflict of interest

The authors declare no conflict of interest.

## References

- Alexander GE, DeLong MR, Strick PL (1986) Parallel organization of functionally segregated circuits linking basal ganglia and cortex. *Annu Rev Neurosci* 9:357–81
- Cavanna AE, Trimble MR (2006) The precuneus: a review of its functional anatomy and behavioural correlates. *Brain* 129:564–83
- De Tieghe X, Goldman S, Laureys S, Verheulpen D, Chiron C, Wetzburger C, Paquier P, Chaigne D, Poznanski N, Jambaque I, Hirsch E, Dulac O, Van Bogaert P (2004) Regional cerebral glucose metabolism in epilepsies with continuous spikes and waves during sleep. *Neurology* 63:853–7
- DeLong MR (2000) The basal ganglia. In: *Principles of Neural Science* (Kandel ER, Schwartz JH, Jessell TM, eds). New York, NY: The McGraw-Hill Companies, 853–67
- Di Martino A, Scheres A, Margulies DS, Kelly AM, Uddin LQ, Shehzad Z, Biswal B, Walters JR, Castellanos FX, Milham MP (2008) Functional connectivity of human striatum: a resting state FMRI study. *Cereb Cortex* 18:2735–47
- Gusnard DA, Raichle ME (2001) Searching for a baseline: functional imaging and the resting human brain. *Nat Rev Neurosci* 2:685–94
- Kim JH, Lee JM, Jo HJ, Kim SH, Lee JH, Kim ST, Seo SW, Cox RW, Na DL, Kim SI, Saad ZS (2009) Defining functional SMA and pre-SMA subregions in human MFC using resting state fMRI: functional connectivity-based parcellation method. *Neuroimage* 49:2375–86

- Krienen FM, Buckner RL (2009) Segregated fronto-cerebellar circuits revealed by intrinsic functional connectivity. *Cereb Cortex* 19:2485–97
- Lipschutz B, Kolinsky R, Damhaut P, Wikler D, Goldman S (2002) Attention-dependent changes of activation and connectivity in dichotic listening. *Neuroimage* 17:643–56
- Marchand WR, Lee JN, Thatcher JW, Thatcher GW, Jensen C, Starr J (2007) Motor deactivation in the human cortex and basal ganglia. *Neuroimage* 38:538–48
- Postuma RB, Dagher A (2006) Basal ganglia functional connectivity based on a meta-analysis of 126 positron emission tomography and functional magnetic resonance imaging publications. *Cereb Cortex* 16:1508–21
- Shoulson I, Fahn S (1979) Huntington disease: clinical care and evaluation. *Neurology* 29:1–3
- Temel Y, Cao C, Vlamings R, Blokland A, Ozen H, Steinbusch HW, Michelsen KA, von Horsten S, Schmitz C, Visser-Vandewalle V (2006) Motor and cognitive improvement by deep brain stimulation in a transgenic rat model of Huntington's disease. *Neurosci Lett* 406:138–41
- Temperli P, Ghika J, Villemure JG, Burkhard PR, Bogouslavsky J, Vingerhoets FJ (2003) How do Parkinsonian signs return after discontinuation of subthalamic DBS? *Neurology* 60:78–81
- Weeks RA, Ceballos-Baumann A, Piccini P, Boecker H, Harding AE, Brooks DJ (1997) Cortical control of movement in Huntington's disease. A PET activation study. *Brain* 120(Part 9):1569–78

Supplementary Information accompanies the paper on the Journal of Cerebral Blood Flow & Metabolism website (<http://www.nature.com/jcbfm>)